On stable Taylor vortices above the transition to wavy vortices

J. Antonijoan
*Department Matemàtica Aplicada IV, Universitat Politècnica de Catalunya, Av. Víctor Balaguer s/n,
08800 Vilanova i la Geltrú, Spain*

J. Sánchez
*Departament Física Aplicada, Universitat Politècnica de Catalunya, c/Gran Capità s/n,
Mod. B5 Campus Nord, 08034 Barcelona, Spain*

The transition from Taylor to wavy vortices is revisited for parameter values in the range of new laboratory experiments [Lin *et al.*, Phys. Fluids **10**, 3233 (1998)]. The dependence of the critical Reynolds number with the axial wavelength of the Taylor vortices is obtained for azimuthal wave numbers from 1 to 5, and for five different values of the radius ratio. We show how islands of stable Taylor vortices above the transition to wavy vortices form. © *2002 American Institute of Physics.*
[DOI: 10.1063/1.1465423]

I. INTRODUCTION

The Taylor–Couette system can exhibit a multiplicity of stable solutions for a given value of the parameters, once the basic Couette flow becomes unstable. Experimental evidence of this behavior has been reported, among other authors, by Coles[1] in 1965. He discovered that different wavy vortex flow states, characterized by their axial and azimuthal wave numbers could be achieved by approaching the final Reynolds number with different accelerations. Jones[2,3] calculated the transition curves from steady axisymmetric Taylor vortices to wavy vortices when both have an axial wavelength of twice the gap between the cylinders, the outer cylinder is at rest and for values of the radius ratio from 0.6 to 1. His results illustrate the complex behavior of these transitions when different radius ratios and azimuthal wave numbers are taken into account. He found that the neutral stability curves allow the existence of stable Taylor vortices above the onset of azimuthal waves in a range of radius ratio between 0.75 and 0.8. This was confirmed experimentally by Park.[4] He found that, for a radius ratio of 0.782 and when the inner Reynolds number is increased quasi-statically, a wavy vortex flow with azimuthal wave number $m=2$ is obtained that returns later to the Taylor vortex state.

The initial wavelength of the Taylor vortices is also an important parameter, which affects the boundaries of the secondary instabilities, as was demonstrated by Mullin and Benjamin[5] and Lorenzen *et al.*[6] We examine here the onset of wavy vortices for a wide range of axial wavelengths, and for systems with five different radius ratios between 0.72 and 0.8. We compare our numerical results with those of Jones,[2] and with the experimental works of Burkhalter and Koschmieder[7] and Lim *et al.*[8] The latter authors studied the effect of the angular acceleration on the critical wavelength of the bifurcated flow and found that stable vortices above the quasi-static transition to wavy vortices can be obtained. These vortices have axial wavelengths shorter than those obtained after a quasi-static transition from Couette flow. We show here that these solutions are connected with the stan-

dard Taylor vortices and that they could also be obtained quasi-statically, for certain values of the radius ratio, if a mechanism of modifying the axial wavelength (as in Ref. 9) is available.

II. THE TAYLOR–COUETTE PROBLEM

We consider the flow of an incompressible fluid confined between two coaxial cylinders. The geometry of the system is specified by the inner and outer radius of the cylinders r_i^* and r_o^*, with gap width $d=r_o^*-r_i^*$. The inner cylinder rotates with angular velocity Ω_i and the outer cylinder is at rest in all the cases we will consider. The nondimensional parameters for the problem are the radius ratio $\eta=r_i^*/r_o^*$, and the inner Reynolds number associated with the tangential velocity of the inner cylinder $R_i=dr_i^*\Omega_i/\nu$, where ν is the kinematic viscosity. We used d as length scale and d^2/ν as time scale. The dimensionless Navier–Stokes equation and the incompressibility condition are then

$$\partial_t\mathbf{v}+\mathbf{v}\cdot\boldsymbol{\nabla}\mathbf{v}=-\boldsymbol{\nabla}p+\Delta\mathbf{v}, \quad \boldsymbol{\nabla}\cdot\mathbf{v}=0. \quad (1)$$

We will assume infinite cylinders and periodic solutions in the axial direction with axial wavelength λ. The boundary conditions are

$$\mathbf{v}=R_i\hat{\mathbf{e}}_\theta \text{ at } r=r_i, \text{ and } \mathbf{v}=0 \text{ at } r=r_o, \quad (2)$$

where r_i and r_o are the dimensionless radii of the cylinders.

III. TAYLOR VORTICES AND THEIR STABILITY

We will only give a brief description of the method we have used to compute the Taylor vortices and to examine their stability. It is fully detailed in Refs. 10 and 11.

We have adopted a formulation based on potentials in which the velocity field is written as

$$\mathbf{v}=f\hat{\mathbf{e}}\theta+h\hat{\mathbf{e}}_z+\boldsymbol{\nabla}\times(g\hat{\mathbf{e}}_\theta+\psi\hat{\mathbf{e}}_z)+\boldsymbol{\nabla}\times\boldsymbol{\nabla}\times(\phi\hat{\mathbf{e}}_z), \quad (3)$$

where f and g depend on (r,z), h depends on (r,θ), and ψ and ϕ depend on the three coordinates (r,θ,z). This velocity

field is divergence-free and the Navier–Stokes equations for velocity and pressure are substituted by the z-components of their curl and double curl written in terms of the potentials. This formulation is general for three-dimensional flows and will be used later to find the eigenvalue problem needed to study the stability of Taylor vortices. In the particular case of Taylor vortices, as they are axisymmetric and the boundaries between cells are flat, (3) can be greatly simplified and the velocity field can be expressed as

$$\mathbf{v}_v(r,z) = f\hat{\mathbf{e}}_\theta + \boldsymbol{\nabla} \times (g\,\hat{\mathbf{e}}_\theta).$$

The system to be solved to find the steady Taylor vortices is

$$\tilde{\Delta}f = -g_z D_+ f + f_z D_+ g,$$

$$\tilde{\Delta}\tilde{\Delta}g = \frac{1}{r}\partial_z f^2 + D_+ g\tilde{\Delta}g_z - g_z D_- \tilde{\Delta}g,$$

with the corresponding boundary conditions

$$f(r_i) = \mathrm{R}_i, \quad f(r_o) = 0, \quad D_+ g = g_z = 0 \quad \text{at} \quad r = r_i, r_o$$

and where the operators are

$$D = \partial_r, \quad D_\pm = D \pm \frac{1}{r}, \quad \tilde{\Delta} = DD_+ + \partial_{zz}^2.$$

In order to solve the equations for the potentials we have used pseudo-spectral methods.[12] The potentials have been expanded using Chebyshev polynomials in the radial direction, and a Fourier expansion in the axial direction. The discretization of the equations for the potentials is obtained by collocation methods in both coordinates. As the Taylor vortex flow is stationary it can be computed using continuation methods varying different parameters. The discretized steady Navier–Stokes equations can be written in the form $F(X,p) = 0$, where p is the continuation parameter R_i or λ. These equations implicitly define a curve of solutions $X = X(p)$ wherever $\det(D_X F(X,p)) \neq 0$. A description of the general continuation techniques can be found in Ref. 13.

The linear stability of the computed Taylor vortices has been studied. We consider non-axisymmetric perturbations of $\mathbf{v}_v$ of the same axial periodicity,

$$\mathbf{v}_p(r,\theta,z,t) = \mathbf{v}_v(r,z) + \mathbf{v}(r,z)e^{\mu t}e^{im\theta}, \qquad (4)$$

$m \in Z$ being the azimuthal wave number of perturbation. In terms of the most general scalar potentials (3),

$$f_p(r,z,t) = f_v(r,z) + f(r,z)e^{\mu t},$$

$$g_p(r,z,t) = g_v(r,z) + g(r,z)e^{\mu t},$$

$$h_p(r,\theta,t) = h(r)e^{im\theta}e^{\mu t},$$

$$\psi_p(r,\theta,z,t) = \psi(r,z)e^{im\theta}e^{\mu t},$$

$$\phi_p(r,\theta,z,t) = \phi(r,z)e^{im\theta}e^{\mu t},$$

where the subscript v refers to the potentials of the Taylor vortex flow. It can be seen[11] that f and g only contribute to axisymmetric instabilities that can be detected during the continuation process to calculate the Taylor vortices. So, we have put $f = g = 0$. In addition the eigenvalue problem can be split into two parts by separating the potentials into its even and odd parts in the vertical coordinate z. If ψ and ϕ are

written as $\psi = \psi^e + \psi^o$ and $\phi = \phi^e + \phi^o$ and after substituting into the equations, a detailed study of the parity of their terms shows that the system can be separated into two kinds of eigenvalue problems. One of them only depends on the potentials ψ^e and ϕ^o and does not disturb the flat boundaries between Taylor vortices. This is the case in the transition of the twisted vortices which appear in a co-rotating system and were studied in Ref. 11. The other eigenvalue problem depends on h, ψ^o, and ϕ^e,

$$\mu h(r) = \Delta_h h(r) - P_z(1-P_\theta)\hat{\mathbf{e}}_z \cdot \mathbf{b}_{h,\psi^o,\phi^e}, \qquad (5)$$

$$\mu \Delta_h \psi^o(r,z) = \Delta\Delta_h \psi^o(r,z) + (1-P_\theta)\hat{\mathbf{e}}_z \cdot \boldsymbol{\nabla} \times \mathbf{b}_{h,\psi^o,\phi^e}, \qquad (6)$$

$$\mu \Delta\Delta_h \phi^e(r,z) = \Delta\Delta\Delta_h \phi^e(r,z)$$
$$- (1-P_\theta)(1-P_z)\hat{\mathbf{e}}_z \cdot \boldsymbol{\nabla} \times \boldsymbol{\nabla} \times \mathbf{b}_{h,\psi^o,\phi^e}, \qquad (7)$$

and corresponds to transitions to wavy solutions in which the boundaries oscillate. In these equations $\Delta_h = D_+ D + 1/r^2 \partial_{\theta\theta}^2$, $\boldsymbol{\omega} = \boldsymbol{\nabla} \times \mathbf{v}$ is the vorticity, P_θ and P_z are the average operators in the two periodic coordinates, and the notation $\mathbf{b}_{h,\psi^o,\phi^e}$ has been used for the term $\mathbf{b} = \boldsymbol{\omega}_u \times \mathbf{v} + \boldsymbol{\omega} \times \mathbf{v}_u$ when the perturbation $\mathbf{v}$ of $\mathbf{v}_v$ is that corresponding to this case:

$$\mathbf{v} = h\hat{\mathbf{e}}_z + \boldsymbol{\nabla} \times (\psi^o\hat{\mathbf{e}}_z) + \boldsymbol{\nabla} \times \boldsymbol{\nabla} \times (\phi^e\hat{\mathbf{e}}_z).$$

The corresponding set of boundary conditions are

$$h = 0, \qquad (8)$$

$$\partial_r \psi^o = \phi^e = \Delta_h \phi^e = 0, \qquad (9)$$

$$m\psi^o + r\partial_{rz}\phi^e = 0, \qquad (10)$$

$$m\Delta\Delta_h \phi^e - rD\Delta_h \partial_z \psi^o = 0, \qquad (11)$$

at $r = r_i, r_o$.

The eigenvalue problem has also been discretized by using the same pseudo-spectral method used to calculate Taylor vortices. The main difficulty is that, in this case, the coupled boundary conditions (10) and (11) make the basis functions for ψ and ϕ to be also coupled. A discrete generalized eigenvalue problem of the form

$$A_m X = \mu_m B_m X$$

is obtained where A_m and B_m are complex matrices which depend on the azimuthal wave number m, and the eigenvector X contains the amplitudes of the eigenfunctions in the aforementioned basis. It is solved by using the subroutine ZGEEV from the LAPACK library.

The code we have developed studies the stability of each solution obtained during the continuation process, and stops when the real part of the leading eigenvalue is zero. The details about the implementation of the spectral methods, the construction of the basis functions verifying the coupled boundary conditions, and the study of the convergence of the critical Reynolds number with the numerical resolution are provided in Ref. 11.
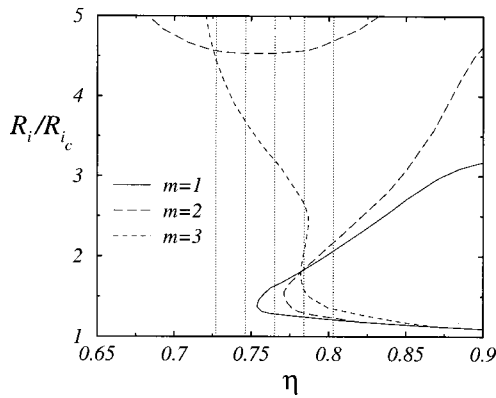
FIG. 1. Neutral curves for the transition to wavy vortices obtained by Jones (Ref. 3).

FIG. 3. As for Fig. 2 with $\eta=0.746\,05$.

IV. RESULTS AND DISCUSSION

Figure 1 shows a detail of the neutral stability curves for the transition of wavy vortices of different m obtained by Jones.[3] The ratio R_i/R_{ic} at which Taylor vortices bifurcate to wavy vortices is plotted against the radius ratio η. R_{ic} is the critical inner Reynolds number for the transition from Couette flow to Taylor vortices. In this figure the axial wavelength of the Taylor vortices is always $\lambda=2d$. The vertical dotted lines indicate the value of the radius ratio (0.727, 0.746 05, 0.7651, 0.784 15, and 0.8032) at which we have studied the dependence of the transition with λ. The former and the latter have been considered in order to compare them with experimental results (Refs. 7 and 8, respectively); the other three are equally spaced between the extreme values. This range corresponds to the region of strong dependence of the transition to wavy vortices with η.

The plots in Figs. 2–6 show the stability boundaries for the onset of wavy vortices of azimuthal wave number m from 1 to 5 in the parameter plane $(\lambda, R_i/R_{ic})$. Each plot corresponds to one of the above-mentioned values of η. The neutral stability curves with azimuthal wave numbers above those of the figures have not been plotted because they are above $R_i/R_{ic}=5$. The numerical resolution used in all calculations has been checked to give accurate results below

this limit (see Ref. 11). Each vertical dotted line at $\lambda=2$ corresponds to one of those of Fig. 1. Their intersections with the neutral curves have been used to compare our results with Jones calculations. We have digitalized his results and the difference in R_i/R_{ic} between both calculations is below 3% for all the aforementioned intersections except for one of them that reaches a 6%. This point corresponds to $m=1$ and $\eta=0.8032$ and, as can be seen in the original figure in Ref. 3, it is difficult to be obtained from the plot because it is very near the intersection with another neutral curve.

For values of $\eta=0.727$ and $\eta=0.746\,05$, the dominant transition is to azimuthal wave number $m=3$ above a certain value of λ. The critical Reynolds number depends strongly on the axial wavelength of the vortices, and for $\lambda>2$ the ratio the ratio R_i/R_{ic} decreases with λ. Below this value, the transition to wavy vortices is above the range of the Reynolds numbers of the plots, leaving a wide region of stable Taylor vortices. Burkhalter and Koschmieder[7] obtained these low-λ solutions in a Taylor–Couette system with $\eta=0.727$, even for R_i/R_{ic} up to 7. In these experiments the inner cylinder
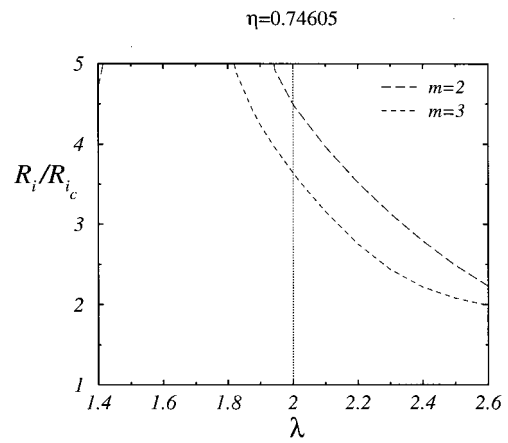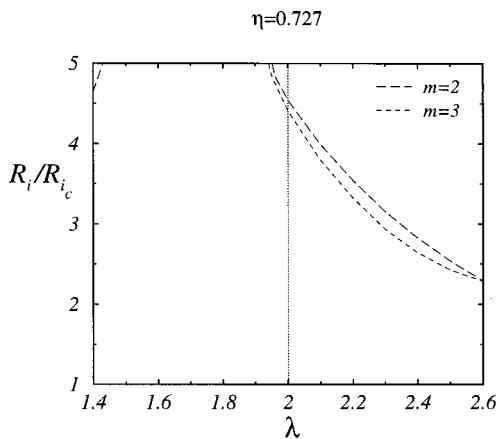

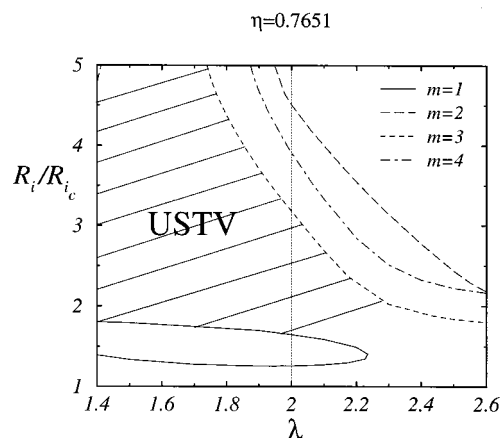FIG. 2. Neutral stability curves for the transition to wavy vortices. $\eta=0.727$.

FIG. 4. Neutral stability curves for the transition to wavy vortices. $\eta=0.7651$. The dashed regions correspond to stable Taylor vortices (USTV).
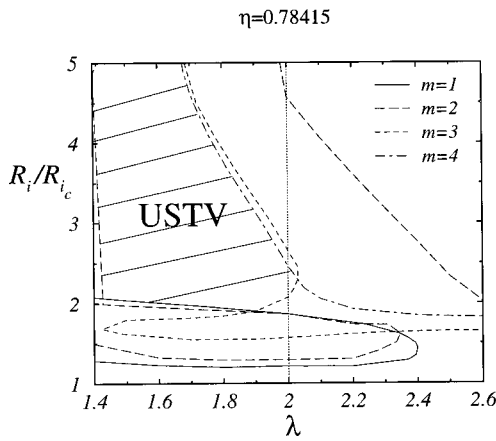
η=0.78415

FIG. 5. As for Fig. 4 with η=0.784 15.

was brought from rest to a supercritical Reynolds number ($R_i > R_{ic}$) in less than 1 s. The minimum λ they obtained is near 1.4 for $R_i/R_{ic} \approx 4$.

When η is increased above 0.75 approximately, a new transition curve of m=1 appears as can be seen in Figs. 1 and 4. This becomes the first instability for a broad range of axial wavelengths. The tongue-shaped curve allows the existence of a region of stable Taylor vortices above it. It has been dashed in Figs. 4–6 and labeled as USTV. It is still connected with the region below the tongue for η=0.7651. In this case the vortices in the dashed region could be obtained quasi-steadily from the standard squared Taylor vortices following a suitable path, if a mechanism of varying the axial wavelength is available (slowly filling or emptying the gap between cylinders, as shown by Snyder,[9] for example).

By further increasing η, new transition curves appear at the turning points of the curves in Fig. 1, with azimuthal wave numbers up to m=5. Some of them have folds which, in the cases m=1 and m=2, grow from left to right as η is increased. For $3 \leq m \leq 5$ they grow in the opposite direction (see Figs. 4–6). Figure 5 shows how the stability curves have separated the region of stable Taylor vortices in two disconnected components. Finally, Fig. 6 shows the situation at η=0.8032. The upper region of stable Taylor vortices

η=0.8032
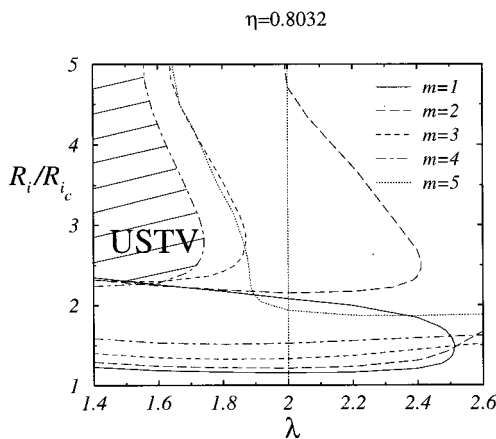

FIG. 6. As for Fig. 4 with η=0.8032.

η=0.8032
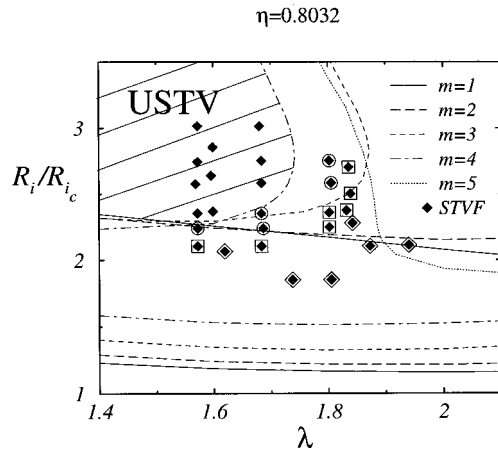

FIG. 7. Detail of the neutral curves for η=0.8032. The diamonds, taken from Lim *et al.* (Ref. 8) correspond to the STVF. Symbols surrounded by circles, squares, and diamonds correspond to different intervals of the maximal growth rate (see text).

(USTV) is now well separated from the lower region by all the transition curves, and it is confined to lower axial wavelengths.

In a recent paper, Lim *et al.*[8] studied the effect of the acceleration of the inner cylinder on the final state in a Taylor–Couette system with η=0.8032, an aspect ratio of 50.54, and a free surface top boundary. When the acceleration (dR_i/dt) is above 2.2 s^{-1}, they found a regime of stable Taylor vortices with axial wavelengths shorter than those obtained quasi-steadily. They refer to it as secondary Taylor vortex flow (STVF). If the acceleration is lower, wavy vortices are obtained in the same range of Reynolds numbers. In Fig. 7 we show a detail of Fig. 6 together with some experimental data obtained from Ref. 8. Each symbol corresponds to one of the solutions found in their study (STVF), with wavelengths between 1.5 and 1.9 and for a range of R_i/R_{ic} form 1.8 to 3.1. They were obtained by accelerating or decelerating the cylinder with 2.2 $s^{-1} \leq |dR_i/dt| \leq 110$ s^{-1}.

If our computational model included all the features of the experiment, all the experimental points would lie inside the dashed region (USTV) of Fig. 7. Actually, or model assumes exact periodicity in the axial direction and so ignores end-effects. It is known that the critical Reynolds numbers for the onset of wavy vortices can be extremely sensitive to variations in the aspect ratio. Although the value in the experiments of Lim *et al.*[8] is high (50.54) the infinite cylinder approximation we use does not reproduce the finite case accurately.

It is usually found in the experiment that the end-effects delay the transition to wavy vortices. Therefore they could be modeled, in a first approximation, by a negative shift of the growth rates we find [$\Re(\lambda)$]. We have computed the spectra at the experimental points outside the stable region (USTV) in Fig. 7 and classified them according to the greater growth rate. The points with maximal growth rate in the intervals (0,0.3), (0.3,0.6), and (0.6,1.1) have been surrounded by a circle, a square, and a diamond, respectively. The more unstable azimuthal wave number is always m=3 or m=4 for all these points.

It can be seen in Fig. 7 that the region delimited by $\Re(\lambda) < \epsilon$ (labeled as USTV when $\epsilon = 0$), which grows with ϵ, includes five more experimental points when $\epsilon = 0.3$ (those surrounded by a circle), and seven more if $\epsilon = 0.6$ (those surrounded by a square). To include all experimental points ϵ must be 1.1. If, as mentioned before, the end-effects are modeled as a maximal negative shift of the growth rates $-\epsilon$, we could obtain the stable region from $\Re(\lambda) < \epsilon$. A shift of $\epsilon = 1.1$ units is then enough to explain the discrepancies between our calculations and the experiments. The value of ϵ could be estimated from the delay in the first transition from Taylor to wavy vortices, but we have not been able to obtain definitive conclusions with the experimental data at hand. Moreover, the growth rates vary very slowly with the Reynolds number (of the order of 2 units for a change of 100 units of the Reynolds number). Therefore, any perturbation of the eigenvalue problem leads to very significant changes in the transition curves. An example of this can be obtained by comparing Figs. 5 and 6. Only a 3% difference in η produces very significant changes; especially in the folds. Another difficulty in comparing our results with the experiments is the way the axial wavelength is measured. In Ref. 8 it is calculated as $\lambda = 2H/Nd$, H being the height of the fluid column, d the gap between the cylinders, and N the number of vortices. The size of the cells, in these experiments, is generally decreasing from top to bottom with a variation of about 3.5%. This does not explain the discrepancies, but shows that the experimental region in which this regime is observed has also some uncertainties. It would be interesting to see if this flow is observed in an apparatus with both ends fixed, and the relationship with our results.

In spite of all the aforementioned comments, Fig. 7 explains the coexistence of the two regimes (Taylor and wavy vortices) observed in the experiments of Lim *et al.*[8] Perturbations of the neutral curves due to the finite length effects, or to the way the axial wavelength is measured, could modify the stability region by embracing more experimental results.

Unfortunately, the study of the transitions to azimuthal dependence with realistic boundary conditions could only be tackled for low values of the aspect ratio due to the complexity of the numerics. We have made calculations with realistic boundary conditions in the vortex breakdown problem in which there is also a discontinuity in the velocity at one of the lids.[14] In that case, we used finite differences and iterative methods based on Krylov subspaces[15] to solve the eigenvalue problems. Spectral methods could also be used if the boundary conditions are regularized and Chebyshev or Legendre expansions are used in the axial coordinate[16] instead of trigonometric functions. We plan to use these techniques for the finite Taylor–Couette problem but, even with this new approach, we do not expect to be able to simulate, in the near future, aspect ratios as large as those we compare with in this article.

ACKNOWLEDGMENTS

[1] D. Coles, "Transition in circular Couette flow," J. Fluid Mech. **21**, 385 (1965).

[2] C. A. Jones, "Nonlinear Taylor vortices and their stability," J. Fluid Mech. **102**, 249 (1981).

[3] C. A. Jones, "The transition to wavy Taylor vortices," J. Fluid Mech. **157**, 135 (1984).

[4] K. Park, "Unusual transition sequence in Taylor wavy vortex flow," Phys. Rev. A **29**, 3458 (1984).

[5] T. Mullin and B. Benjamin, "Transition to oscillatory motion in the Taylor experiment," Nature (London) **288**, 567 (1980).

[6] A. Lorenzen, G. Pfister, and T. Mullin, "End effects on the transition to time-dependent motion in the Taylor experiment," Phys. Fluids **26**, 10 (1983).

[7] J. E. Burkhalter and E. L. Koschmieder, "Steady supercritical Taylor vortices after sudden starts," Phys. Fluids **17**, 1929 (1974).

[8] T. T. Lim, Y. T. Chew, and Q. Xiao, "A new flow regime in a Taylor–Couette flow," Phys. Fluids **10**, 3233 (1998).

[9] H. A. Snyder, "Wave-number selection at finite amplitude in rotating Couette flow," J. Fluid Mech. **35**, 273 (1969).

[10] F. Marques, "On boundary condition for velocity potentials in confined flows: Application to Couette flow," Phys. Fluids A **2**, 729 (1990).

[11] J. Antonijoan and J. Sánchez, "Transitions from Taylor vortex flow in a co-rotating Taylor–Couette system," Phys. Fluids **12**, 3147 (2000).

[12] C. Canuto, M. Y. Hussaini, A. Quarteroni, and T. A. Zang, *Spectral Methods in Fluid Dynamics* (Springer-Verlag, New York, 1987).

[13] Y. Kuznetsov, *Elements of Applied Bifurcation Theory* (Springer, New York, 1998).

[14] J. M. Lopez, F. Marques, and J. Sánchez, "Oscillatory modes in an enclosed swirling flow," J. Fluid Mech. **439**, 109 (2001).

[15] W. S. Edwards, L. S. Tuckerman, R. A. Friesner, and D. S. Sorensen, "Krylov methods for the incompressible Navier–Stokes equations," J. Comput. Phys. **110**, 82 (1994).

[16] J. M. Lopez and J. Shen, "An efficient spectral-projection method for the Navier–Stokes equations in cylindrical geometries," J. Comput. Phys. **139**, 1 (1998).